Expression Profiles of NOD-Like Receptors and Regulation of NLRP3 Inflammasome Activation in Toxoplasma Gondii-Infected Human Small Intestinal Epithelial Cells

Jia-Qi CHu
Guangdong Medical University
Fei Fei Gao
Chungnam National University
Weiyun Wu
Guangdong Medical College Zhanjiang Campus: Guangdong Medical University
Chunchao Li
Guangdong Medical University
Zhaobin Pan
Guangdong Medical University
Jinhui Sun
Guangdong Medical University
Hao Wang
Guangdong Medical University
Cong Huang
Peking University Shenzhen Hospital
Sang Hyuk Lee
Sun General Hospital: Daejeon Sun Hospital
Juan-Hua Quan
Guangdong Medical University
Young-Ha Lee (yhalee@cnu.ac.kr)
Chungnam National University School of Medicine

Research

Keywords: Toxoplasma gondii, Human small intestinal epithelial cells, NOD-like receptors, inflammasome, Caspase-cleaved interleukins

Posted Date: December 23rd, 2020

DOI: https://doi.org/10.21203/rs.3.rs-133332/v1

Version of Record: A version of this preprint was published on March 12th, 2021. See the published version at https://doi.org/10.1186/s13071-021-04666-w.

Abstract

Background: *Toxoplasma gondii* is a parasite that majorly infects through the oral route. Nucleotide-binding oligomerization domain (NOD)-like receptors (NLRs) play crucial roles in the immune responses generated during the parasitic infection and also drive the inflammatory response against invading parasites. However, little is known about the regulation of NLRs and inflammasome activation in *T. gondii*-infected human small intestinal epithelial (FHs 74 Int) cells.

Methods: FHs 74 Int cells infected with *T. gondii* were subsequently evaluated for morphological changes, cytotoxicity, expression profiles of NLRs, inflammasome components, caspase-cleaved interleukins (ILs), and the mechanisms of NLRP3 and NLRP6 inflammasome activation. Immunocytochemistry, lactate dehydrogenase assay, reverse transcription polymerase chain reaction (RT-PCR), real-time quantitative RT-PCR, and western blotting techniques were utilized for the analysis purpose.

Results: Under normal and *T. gondii*-infected conditions, members of the NLRs, inflammasome components, and caspase-cleaved ILs were expressed in the FHs Int 74 cells, except for NLRC3, NLRP5, and NLRP9. Among the NLRs, mRNA expression of *NOD2*, *NLRP3*, *NLRP6*, and *NAIP1* were significantly increased in *T. gondii*-infected cells, whereas that of *NLRP2*, *NLRP7*, and *CIITA* mRNAs decreased significantly in a time-dependent manner. In addition, *T. gondii* infection induced NLRP3, NLRP6 and NLRC4 inflammasome activation and production of IL-1β, IL-18, and IL-33 in FHs 74 Int cells. *T. gondii*-induced NLRP3 inflammasome activation was strongly associated with the phosphorylation of p38 MAPK but not JNK1/2. NLRP6 inflammasome activation was not related to the MAPK pathway in FHs 74 Int cells.

Conclusions: This study highlighted the expression profiles of NLRs and unraveled the underlying mechanisms of NLRP3 inflammasome activation in *T. gondii*-infected FHs 74 Int cells. These findings may contribute to understanding of the mucosal and innate immune responses induced by the NLRs and inflammasomes during *T. gondii* infection in FHs 74 Int cells.

Background

Toxoplasma gondii is an obligate intracellular protozoan parasite that infects one-third of the world's population [1]. Infection is most commonly acquired through the ingestion of raw or undercooked meat containing the cystic bradyzoite form of *T. gondii* or through the ingestion of materials contaminated with cat feces that may contain *T. gondii* oocysts. Once inside the body, the parasite breaches the intestinal epithelial barrier and spreads from the lamina propria to other organs [2]. Intestinal epithelial cells can sense and respond to the invading microbial stimuli to reinforce their barrier function. They also participate in the coordination of appropriate immune responses [3]. The innate immune system plays a significant role in sensing pathogens and triggering biological mechanisms to control infection and eliminate pathogens [4, 5]. It is activated when pattern recognition receptor proteins, such as Toll-like receptors (TLRs) or nucleotide-binding oligomerization domain (NOD)-like receptors (NLRs), detect the presence of pathogens, their products, or the danger signals [5–7].

NLR are a large group of cytosolic sensors that have diverse functions in innate immunity and inflammation. Based on the type of N-terminal domain, NLRs are classified into four subfamilies, NLRA, NLRB, NLRC, and NLRP and an additional subfamily, NLRX1 [7, 8]. Several NLR molecules remain associated with the *T. gondii*-infection mediated immune responses in the infected hosts. It has been reported that *NOD2*-deficient mice are unable to clear *T. gondii* and fail to induce an appropriate adaptive immune response [9]. In addition to NOD2, NLRP1b and NLRP3 are also involved in rendering protection against *T. gondii* infection [10, 11]. In human acute monocytic leukemia cell line macrophages, the messenger RNA (mRNA) levels of *NLRC4*, *NLRP6*, *NLRP8*, *NLRP13*, *AIM2*, and *NAIP* are significantly elevated due to *T. gondii* infection, in a time-dependent manner [12]. Although some studies involving mice or cell lines have reported the involvement of NLR members in *T. gondii* infection protection [9–12], little information is available about the regulation of NLR activation in gut epithelial cells.

Ligand recognition by the NLR family members, such as NLRP1, NLRP3, NLRP6, NLRP12, and NLRC4 leads to the activation of inflammasome, a multiprotein complex, which cleaves interleukin (IL)-1β, IL-18, IL-33, and IL-37 (IL-17A) by caspases, the effector components of inflammasomes [8, 10–14]. *T. gondii* infection in cells with *NLRP1* knockdown fails to induce the production of inflammatory cytokines including IL-1β, IL-18, and IL-12 compared to control cells [10]. The broad range of

pathogens that act on NLRP3 in several kinds of epithelial cells, include *Plasmodium* sp., *Trypanosoma cruzi*, *Leishmania* sp., and *T. gondii* [15]. The P2 × 7R/NLRP3 pathway plays an important role in IL-1β secretion and inhibition of *T. gondii* proliferation in small intestinal epithelial cells [16]. While reports have revealed NLR activation by *T. gondii* infection in various cells, information on inflammasome activation in gut epithelial cells infected with *T. gondii* is very scarce.

NLRs play a crucial role in inducing immune responses during parasitic infection and driving the inflammatory responses against invading parasites. However, little is known about the regulation of NLRs and NLR-related inflammasome activation in *T. gondii*-infected human small intestinal epithelial (FHs 74 Int) cells. Therefore, this study evaluated the expression profiles of NLRs, inflammasome components, and caspase-cleaved ILs and investigated the mechanisms of some popular inflammasomes' activation in *T. gondii*-infected FHs 74 Int cells.

Methods

Cell culture

A non-transformed human fetal small intestinal epithelial cell line (FHs 74 Int cells) was purchased from ATCC (ATCC, Manassas, VA, USA) and cultured in DMEM with 10% (v/v) heat-inactivated fetal bovine serum (FBS), an antibiotic-antimycotic solution, and 30 ng/ml human epidermal growth factor (all from Gibco, Grand Island, NY, USA) at 37 °C in a humidified atmosphere at 5% (v/v) CO_2. The medium was changed every 2–3 days.

Maintenance of T. gondii

Tachyzoites of the *T. gondii* RFP-RH or RH strain were maintained as described previously [16]. Briefly, human retinal pigment epithelial cells (ARPE-19 cells) (ATCC) were cultured in a 1:1 (v/v) mixture of DMEM/F12 supplemented with 10% (v/v) FBS and an antibiotic-antimycotic solution (all from Gibco). ARPE-19 cells were infected with *T. gondii* at a multiplicity of infection (MOI) of 5 for 2–3 days. After spontaneous host cell rupture, parasites and cellular debris were pelleted by centrifugation and washed in cold PBS. The final pellet was resuspended and passed through a 26-gauge needle fitted with a 5.0 μm pore-sized filter (Millipore, Billerica, MA, USA).

Reverse transcription polymerase chain reaction (RT-PCR)

Total RNA was extracted using TRIzol Reagent (Invitrogen, Carlsbad, CA, USA) and RNA was transcribed into cDNA using M-MLV reverse transcriptase (Invitrogen) as described by the manufacturer. Polymerase chain reaction (PCR) was performed with TaKaRa Ex Taq (Takara Bio, Shiga, Japan) in reactions containing 33.75 μL distilled water, 5 μL 10 × Ex Taq buffer, 4 μL dNTP mixture (2.5 mM each), 2 μL of each primer, 0.25 μL of TaKaRa Ex Taq, and 3 μL of template cDNA to total 50 μL. PCR amplification conditions were an initial denaturation at 95 °C for 5 min, followed by 35 cycles of 95 °C for 30 s, an annealing 60 °C for 30 s and an extension step of 72 °C for 30 s. Finally, PCR was completed with the additional extension step for 10 min. The PCR products were analyzed on 1.5% agarose gel in 0.5× TBE buffer and visualized using ethidium bromide and UV transilluminator. The details of primers designed are presented in Table 1.

Table 1
Members of the NLR family, inflammasome components and caspase-cleaved interleukins, and primers used to investigate their expressions by RT-PCR and qRT-PCR.

Family	Name	Synonym	Forward 5'-3'	Reverse 5'-3'	Amplicon length (bp)
NLRC	NOD1	CARD4	ACTGAAAAGCAATCGGGAACT	ACACACAATCTCCGCATCTTC	112
	NOD2	CARD15	GCCTGATGTTGGTCAAGAAGA	GATCCGTGAACCTGAACTTGA	107
	NLRC3	NOD3, CLR16.2	GGAGCCTCACCAGCTTAGATT	AGGCCACCTGGAGATAGAGAG	117
	NLRC4	IPAF, CARD12	GGAAAGTGCAAGGCTCTGAC	TGTCTGCTTCCTGATTGTGC	129
	NLRC5	NOD27, CLR16.1	CACCCTGACCAACATCCTAGA	TCTCTATCTGCCCACAGCCTA	113
NLRP	NLRP1	NALP1, CARD7	ATACGAAGCCTTTGGGGACT	ACAAAGCAGAGACCCGTGTT	148
	NLRP2	NALP2	CACCGAATGGATCTGTCTGA	GTGGTCGTTCTTTCCGTGTT	112
	NLRP3	NALP3, CIAS1	AAAGGAAGTGGACTGCGAGA	TTCAAACGACTCCCTGGAAC	129
	NLRP4	NALP4	CCAACGAGTTTGGCTGACTT	GCTGTCGATGACGAACAAGA	105
	NLRP5	NALP5	CTGGGGAACGAAGGTGTAAA	GCAAGTGCAAGAAAACCACA	122
	NLRP6	NALP6	CTGTTCTGAGCTACTGCGTGAG	AGGCTCTTCTTCTTCTTCTCCTG	100
	NLRP7	NALP7	TAACCCGTAGCACCTGTCATC	GGTCTTCTTCCCAATGAAAGC	101
	NLRP8	NALP8	CGCTGGTGTGCTTTCTACTTC	GGTCGGGTTTGGACATAATCT	130
	NLRP9	NALP9	CTAGCCTCTCCCAGTCTGACAT	GCGATGTCTTCACAAACTTCAC	121
	NLRP10	NALP10	GTCACGGTGGAGGCTCTATTT	CGAGAGTTGTCTTTCCAGTGC	100
	NLRP11	NALP11	GTGTTGCATGTGACGTTTCC	TTTTGTTGCTCCCAATCTCC	157
	NLRP12	NALP12	CGACCTTTACCTGACCAACAA	AGGTCCATCCCAAATAACCAG	114
	NLRP13	NALP13	ATGGTGTGTTGGACCGTATGT	GCCAAATCTACCTCTGCTGT	140
	NLRP14	NALP14	CCGCTTGTACTTGTCTGAAGC	GCCTCCATCTACTGGTGTGAA	122
NLRB	NAIP1	BIRC1, NLRB1	AGTACTTTTTCGACCACCCAGA	TAGTTGGCACCTGTGATTTGTC	135
NLRA	CIITA	MHC2TA, C2TA	CCGACACAGACACCATCAAC	CCTCTGGGAAGGGTCTTTTC	249
NLRX	NLRX1	NOD9	TGGCCTTGTCTCAGCTCTTTA	CACCAGTCCAGAACCATCTTG	121
Infl. comp.	Caspase 1	IL1BC	GGGGTACAGCGTAGATGTGAA	CTTCCCGAATACCATGAGACA	137
	Caspase 5	ICH-3	TCTGTTTGCAAGATCCACGA	GTTCTATGGTGGGCATCTGG	223
	Caspase 8	ALPS2B	AGAAGAGGGTCATCCTGGGAGA	TCAGGACTTCCTTCAAGGCTGC	142
	ASC	PYCARD	CTGACGGATGAGCAGTACCA	CAAGTCCTTGCAGGTCCAGT	108

Family	Name	Synonym	Forward 5′-3′	Reverse 5′-3′	Amplicon length (bp)
Interleukins	IL-1β	IL1F2	CCACAGACCTTCCAGGAGAA	GTGATCGTACAGGTGCATCG	121
	IL-18	IL1F4	CACCCCGGACCATATTTATT	TCATGTCCTGGGACACTTCTC	205
	IL-33	IL1F11	GGTGACGGTGTTGATGGTAAG	CTGGCAGTGGTTTTTCACACT	121
	IL-37	IL-1F7	CAGCCTCTGCGGAGAAAGGAAGT	GTTTCTCCTTCTTCAGCTGAAGG	120
Control	HPRT1	HGPRT	GACCAGTCAACAGGGGACAT	CTGCATTGTTTTGCCAGTGT	111

Immunocytochemistry

FHs 74 Int cells were seeded onto coverslips in 12-well plates at a density of 1×10^4 cells/well and incubated for 24 h. The cells were infected with *T. gondii* at MOI 10 for 0, 4 and 8 h. Subsequently, the cells were washed with Hank's balanced salt solution (HBSS) and fixed with freshly prepared 4% paraformaldehyde for 1 h at room temperature. After washing five times with PBS containing 0.3% Triton X-100 (PBS-T) for 10 min, the cells were incubated with primary antibodies (α-tubulin, cleaved caspase-8, cleaved IL-1β, IL-33) for 2 h at room temperature. The cells were washed to remove excess primary antibody, and then incubated with the appropriate fluorescently labeled secondary antibodies (anti-mouse Alexa Fluor 647, anti-rabbit Alexa Fluor 647, anti-mouse Alexa Fluor 488 and anti-rabbit Alexa Fluor 488) for 2 h at room temperature. After mounting with VECTASHIELD HardSet antifade mounting medium with DAPI (Vector Laboratories, Burlingame, CA, USA), fluorescence images were acquired using a confocal microscope (Leica, Wetzlar, German).

Lactate dehydrogenase (LDH) assay

LDH assay was performed to quantify cytotoxicity. This assay was conducted using the CytoTox 96 Non-Radioactive Cytotoxicity Assay kit (Promega) according to the manufacturer's protocol. Briefly, 1×10^4 cells were seeded into 96-well plates and infected with *T. gondii* MOI 10 for 0, 4 and 8 h in an incubator (5% CO_2, 90% relative humidity, 37 °C). Next, 50 µL of the supernatant was transferred into a new 96-well plate and 50 µL of CytoTox 96 reagent was added and incubated for 30 min at room temperature. After incubation, the absorbance of the solution was measured immediately at 490 nm using a microplate reader (TECAN, Männedorf, Switzerland). LDH levels in the media were quantified and compared to control values according to the kit instructions.

Real-time quantitative reverse transcription polymerase chain reaction (qRT-PCR)

qRT-PCR was performed using Power SYBR® Green PCR Master Mix (Applied Biosystems, Foster City, CA, USA). The primers used in this study are summarized in Table 1. All reactions were performed with an ABI 7500 Fast Real-Time PCR system (Applied Biosystems, Carlsbad, CA, USA) under the following conditions: 95 °C for 30 s, followed by 40 cycles of 95 °C for 15 s and 60 °C for 30 s. Relative gene expression levels were quantified based on the cycle threshold (Ct) values and normalized to the reference gene hypoxanthine phosphoribosyltransferase 1 (HPRT1). Each sample was measured in triplicate, and the gene expression levels were calculated using the $2^{-\Delta\Delta Ct}$ method.

Western blotting

FHs 74 Int cells were infected with *T. gondii* at MOI 10 for 0, 4 and 8 h. FHs 74 Int cells were preincubated with the 30 µM of SB203580 (p38 MAPK inhibitor) and SP600125 (JNK1/2 inhibitor) for 2 h and infected with *T. gondii* MOI 10 for a further 8 h. Subsequently, cell lysates were collected and lysed in ice-cold radio-immunoprecipitation assay (RIPA) buffer (Thermo Fisher Scientific, Grand Island, NY, USA). Protein concentrations were determined using the Bradford assay (Bio-Rad, Hercules, CA, USA). Total protein (30 µg) was resolved on 10–12% SDS-PAGE gels and then transferred to PVDF membranes (Merck Millipore, Billerica, MA, USA). The membranes were blocked with 5% nonfat skim milk in TBS containing 0.1% Tween 20 (TBST)

for 1 h and incubated with primary antibodies against TP3, NLRP1, NLRP3, NLRP6, NLRC4, NAIP1, cleaved caspase-1, ASC, cleaved IL-1β, IL-33, p-p38 MAPK, p38 MAPK, p-ERK1/2, ERK1/2, p-JNK1/2, JNK1/2 and α-Tubulin overnight at 4 °C. Subsequently, the membranes were incubated with HRP-conjugated secondary antibody (Santa Cruz Biotechnology) for 2 h at room temperature. The membrane was soaked with Immobilon Western Chemiluminescent HRP Substrate (Jackson ImmunoResearch Laboratories), and chemiluminescence was detected with a Fusion Solo System (Vilber Lourmat, Collegien, France). Band intensity was quantified using ImageJ software (NIH, Bethesda, MD, USA). The results were normalized to α-tubulin or β-tubulin protein levels and are expressed as fold-changes compared to the control group.

ELISA

FHs 74 Int cells were infected with *T. gondii* at MOI 10 for 0, 4 and 8 h. The supernatants from the mock- or *T. gondii*-infected FHs 74 Int cells were collected in triplicate, and IL-1β and IL-18 levels were measured using commercially available ELISA kits following the manufacturer's instructions (R&D System, Minneapolis, Minnesota, USA). The cytokine concentrations in the samples were calculated from standard curves obtained using recombinant cytokines.

Statistical analysis

All results are presented as the means ± standard deviations (SDs) of at least three independent experiments, unless otherwise indicated. Statistical comparisons were carried out using GraphPad Prism software (GraphPad Software Inc., San Diego, CA, USA) and the multiple t tests was used to determine one-way ANOVA procedures. Differences were considered significant at $P < 0.05$.

Results

Expression of NLRs, inflammasome components, and caspase-cleaved ILs in FHs 74 Int cells

We first checked the expression of the 22 known members of the human NLR family (Table 1) in FHs 74 Int cells using RT-PCR. Our results indicated that majority of the NLR family members, including NOD1, NOD2, NLRC4, NLRC5, NLRP1, NLRP2, NLRP3, NLRP4, NLRP6, NLRP7, NLRP8, NLRP10, NLRP11, NLRP12, NLRP13, NLRP14, NAIP1, CIITA, and NLRX1 were expressed in these cells under normal conditions (Fig. 1A). After normalization with housekeeping gene HPRT 1, NLRP1 and NOD1 were identified as the most abundantly expressed NLRs in FHs 74 Int cells (Fig. 1B). For primer functionality tests, we used different cell types of human origin that are known to express the respective NLRs and detected the expression of *NLRC3*, *NLRP5*, and *NLRP9* mRNAs (Fig. 1C). Furthermore, we examined the presence of various inflammasome components and ILs cleaved by caspases. Our results revealed that caspase-1, caspase-5, caspase-8, and ASC inflammasome components and IL-1β, IL-18, IL-33, and IL-37 were expressed in the FHs 74 Int cells (Fig. 1D).

Effects of T. gondii infection on cell morphology and cytotoxicity of FHs 74 Int cells

FHs 74 Int cells were incubated with *T. gondii* at MOI of 10 for various time periods. The integrity of the microtubule network was assessed with immunofluorescence microscopy using α-tubulin antibody and DAPI for staining cellular microtubules and DNA, respectively. As shown in Fig. 2A, the cell nucleus (blue) was wrapped with a well-developed array of hair-like microtubule networks of slim fibrous microtubules (red) in control cells. In contrast, the α-tubulin staining patterns were diffuse and disorganized in *T. gondii*-infected FHs 74 Int cells. The number of *T. gondii*-infected cells and the total number of cells were counted under a fluorescence microscope. *T. gondii* infection rate significantly increased in an infection time-dependent manner (73.1% at 4 h and 89.5% at 8 h).

Furthermore, to investigate *T. gondii*-induced cytotoxicity of FHs 74 Int cells, the cells were incubated with *T. gondii* at an MOI of 10 for 0, 4, and 8 h. Post-incubation, LDH assay was performed. Release of LDH significantly increased in the *T. gondii*-infected groups compared to that in the mock-infected control group. Cytotoxicities of FHs 74 Int cells infected with *T. gondii* for 0, 4,

and 8 h were 4.34 ± 0.15%, 19.21 ± 1.88%, and 40.02 ± 1.57%, respectively (Fig. 2B). These data indicate that *T. gondii* infection induces morphological disorganization and cytotoxicity in FHs 74 Int cells in an infection time-dependent manner.

Transcriptional regulation of NLRs in FHs 74 Int cells

Next, we aimed to investigate the expression of the identified NLRs in response to *T. gondii* infection for 4 or 8 h. Real-time qRT-PCR revealed that *T. gondii* infection induces a significant time-dependent increase in the expression of *NOD2*, *NLRP3*, *NLRP6*, and *NAIP1* mRNAs (Fig. 3A). Interestingly, *T. gondii* infection upregulated the expression of *NLRC4*, *NLRP4*, *NLRP8*, *NLRP10*, *NLRP11*, *NLRP13*, and *NLRP14* mRNAs at both 4 and 8 h post-infection, but *NLRP4*, *NLRP8*, *NLRP10*, and *NLRP11* mRNAs were significantly downregulated at 8 h post-infection compared to that at 4 h post-infection (Fig. 3B). In contrast, *T. gondii* infection induced a time-dependent significant decrease in the expression of *NLRP2*, *NLRP7*, and *CIITA* mRNAs (Fig. 3C). No significant changes in the expression of *NOD1*, *NLRC3*, *NLRC5*, *NLRP1*, *NLRP9*, *NLRP12*, and *NLRX1* mRNAs were noted as a result of *T. gondii* infection (data not shown). Neither normal nor *T. gondii*-infected FHs 74 Int cells expressed *NLRP5* mRNA. While *T. gondii* infection increased the expression of mRNAs encoding caspase-1, ASC, IL-1β, IL-18, and IL-33, it had no effect on the expression of mRNAs encoding caspase-5, caspase-8, and IL-37(Fig. 3D). These results clearly indicate that *T. gondii* infection activates NLRs, but their expression patterns vary in FHs 74 Int cells.

T. gondii infection induced NLRP3, NLRP6, and NLRC4 inflammasome components in FHs 74 Int cells

Until now, the most commonly studied inflammasomes in protozoan parasites were NLRP1, NLRP3, and NLRC4 [15]. Thus, we further investigated the protein levels of NLRP1, NLRP3, NLRP6, and NLRC4 inflammasome components in response to *T. gondii* infection. *T. gondii* infection time-dependently induced NLRP3 and ASC protein expression, adequately induced NLRP6 and cleaved caspase-1 expression, and moderately induced NLRC4 expression at 4 h post-infection. However, expression levels for NLRP1 and NAIP1 proteins remained unchanged in response to *T. gondii* infection (Fig. 4A). Confocal microscopy revealed that the expression of cleaved caspase-8 was higher in *T. gondii*-infected FHs 74 Int cells compared to that in mock-infected control FHs 74 Int cells (Fig. 4B). These results indicate that *T. gondii* infection induces NLRP3, NLRP6, and NLRC4 inflammasome activation in FHs 74 Int cells.

T. gondii infection upregulates IL expression and release in FHs 74 Int cells

NLRs are a large group of cytosolic sensors whose main function is to modulate the expression of proinflammatory cytokines [8, 10–14]. Hence, we evaluated the protein expression levels of IL-1β, IL-18, IL-33, and IL-37 in *T. gondii*-infected FHs 74 Int cells. Western blot analysis results revealed upregulated expression of cleaved IL-1β, cleaved IL-18, and IL-33 proteins in the *T. gondii*-infected FHs 74 Int cell lysates (Fig. 5A). The concentrations of released IL-1β and IL-18 were measured in the *T. gondii*-infected FHs 74 Int cell culture medium. *T. gondii* infection induced a robust increase in the amount of active IL-1β and IL-18 in the culture medium (Fig. 5B). Confocal microscopy detected similar expression levels of cleaved IL-1β and IL-33. In control cells, cleaved IL-1β levels were non-detectable, while in *T. gondii*-infected cells, activated IL-1β and IL-33 increased significantly (Fig. 5C and D). These results indicate that *T. gondii* induces IL-1β, IL-18, and IL-33 production in FHs 74 Int cells.

T. gondii -induced NLRP3 inflammasome activation remains strongly associated with phosphorylation of p38 MAPK

Previous studies have reported that mitogen-activated protein kinase (MAPK) pathway remains associated with inflammasome activation [17–19]. Hence, we investigated the involvement of MAPK pathway in *T. gondii*-induced NLRP3 and NLRP6 inflammasome activation. As shown in Fig. 6A, T. *gondii* infection increased the levels of phosphorylated p38 MAPK and JNK1/2; however, phosphorylated ERK1/2 levels decreased compared to that in the control cells. No significant changes in the total protein levels of ERK1/2, p38 MAPK, and JNK1/2 were observed after *T. gondii* infection. However, on pretreatment with SB203580 (p38 inhibitor) and SP600125 (JNK inhibitor), phosphorylation levels of p38 MAPK and JNK1/2 significantly decreased in the *T. gondii*-infected cells compared to that in inhibitor-untreated *T. gondii*-infected cells. Interestingly, pretreatment with SB203580 significantly downregulated the *T. gondii*-infection induced NLRP3 expression. However, NLRP3 levels in inhibitor-untreated *T. gondii*-infected cells were similar to those in the *T. gondii*-infected group pre-treated with SP600125. In addition, pretreatment with SB203580 and SP600125 had no effect on the *T. gondii*-infection regulated NLRP6

and cleaved caspase-1 protein expression. Undoubtedly, SB203580 and SP600125 pretreatment significantly attenuated the *T. gondii*-infection induced elevated levels of cleaved IL-1β and cleaved IL-18 (Fig. 6B). These results indicate that *T. gondii*-infection induced NLRP3 inflammasome production in FHs 74 Int cells remains strongly associated with the activation of the p38 MAPK, but not JNK1/2 signaling pathways (Fig. 7).

Discussion

This study revealed that members of the NLRs, inflammasome components, and caspase-cleaved ILs are expressed differently in the FHs Int 74 cells under normal and *T. gondii*-infected conditions, however NLRC3, NLRP5, and NLRP9 were not expressed. The most abundantly expressed NLRs were NLRP1 and NOD1. *T. gondii* infection induced cytotoxicity in FHs 74 Int cells in an infection time-dependent manner. In addition, the expression of *NOD2*, *NLRP3*, *NLRP6*, and *NAIP1* mRNAs significantly increased in *T. gondii*-infected cells, while that of *NLRP2*, *NLRP7*, and *CIITA* mRNAs decreased. *T. gondii* infection also induced NLRP3, NLRP6 and NLRC4 inflammasome activation and significantly produced IL-1β, IL-18, and IL-33 in FHs 74 Int cells. NLRP3 inflammasome activation was strongly associated with p38 MAPK pathway in *T. gondii*-infected cells; however, no relationship was revealed between NLRP6 inflammasome activation and MAPK pathway.

Expression of the NLR family as a pattern recognition receptor is cell specific, however, little was known about the regulation of NLRs and their activation mechanisms in intestinal epithelial cells. In this study, the expression patterns of the NLRs, inflammasome components, and caspase-cleaved ILs were varied in the FHs Int 74 cells under normal and *T. gondii*-infected conditions. Although a previous study reported the expression patterns of NLRs in cerebral endothelial cells [8], this is the first study about the regulation of whole NLRs in the human intestinal cells after *T. gondii* infection. NLRs can be regulated by a wide range of cellular damages, including oxidative stress and inflammatory stimuli [5, 7]. Thus, upon evaluating the cellular changes in *T. gondii*-infected FHs 74 Int cells by immunofluorescence and LDH assay, we observed disorganized staining patterns for α-tubulin and significantly increased release of LDH in proportion to time. These results clearly indicated that *T. gondii* infection induces cellular damage and cytotoxicity in FHs 74 Int cells by activation of inflammasome-related components. Similar phenomena were observed for *Schistosoma mansoni* infection, wherein elicited host immune responses resulted in mitochondrial damage, generation of high levels of reactive oxygen species (ROS), and activation of apoptosis through interaction with host inflammasomes [20]. In addition, *Neospora caninum*-induced NADPH-dependent ROS generation plays an important role in NLRP3 inflammasome activation [21].

On investigating the activation process of some well-known inflammasomes in *T. gondii*-infected FHs 74 Int cells, we observed that *T. gondii* infection induces the expression of NLRP3, ASC, NLRP6, NLRC4, cleaved caspase-1, and cleaved caspase-8 proteins. In addition, increased production of ILs, such as IL-1β, IL-18, and IL-33 was also noted in *T. gondii*-infected FHs 74 Int cells. Thus, it was suggested that *T. gondii* infection induces activation of NLRP3, NLRP6 and NRC4 inflammasomes through the recruitment of ASC and caspases and production of proinflammatory cytokines in FHs 74 Int cells. These findings were partly consistent with previous reports that detected NLRP3, ASC, caspase-1, and IL-1β in *T. gondii*-infected mice [11]. Lipopolysaccharide/adenosine triphosphate induced IL-1β and IL-18 secretion through the NLRP3 inflammasome activation in RAW264.7 murine macrophage cells [22] and high glucose and lipopolysaccharide primed NLRP3 inflammasome via the ROS/thioredoxin-interacting protein pathway in mesangial cells resulted in the cleavage of procaspase-1 and activation of cytokines IL-1β, IL-18, and IL-33 [23].

MAPKs, highly conserved in all eukaryotes, control a variety of cellular processes, including cell differentiation, proliferation, survival, and stress responses. It has been reported that the MAPK pathway remains associated with inflammasome activation [17–19]. We evaluated the roles of MAPK signaling pathways in NLRP3 and NLRP6 inflammasome activation by subjecting the *T. gondii*-infected FHs 74 Int cells to pretreatment with SB203580 and SP600125, inhibitors of p38 MAPK and JNK, respectively. While SB203580 pretreatment significantly downregulated the *T. gondii*-induced expression of NLRP3, cleaved IL-1β, and cleaved IL-18, SP600125 pretreatment had no effect on NLRP3 and NLRP6 expression. These findings suggested that NLRP3 inflammasome activation remains strongly associated with the phosphorylation of p38 MAPK and not JNK1/2 in *T. gondii*-infected FHs 74 Int cells; however, NLRP6 inflammasome activation had no correlation with MAPK pathway. Our results were consistent with a previous study that reported p38 MAPK is critically important for the regulation of NLRP1 or NLRP3

inflammasome activation and IL-1β secretion [18, 19]. Wang et al. [24] reported that *T. gondii* infection and MAPKs are associated with the inflammasome activation in mice.

Conclusion

We demonstrated the regulation of NLRs and NLR-related inflammasome activation in *T. gondii*-infected human small intestinal epithelial (FHs 74 Int) cells. *T. gondii* infection induce the expression of NLRs, inflammasome components, and caspase-cleaved ILs in the FHs Int 74 cells, but their expression patterns were varied. NLRP3 inflammasome activation was strongly associated with the p38 MAPK pathway; however, NLRP6 inflammasome activation had no correlation with MAPK pathway. We believe that the study findings would contribute to the understanding of mucosal and innate immune responses induced by NLRs and inflammasomes in *T. gondii*-infected FHs Int 74 cells.

Abbreviations

BSA: bovine serum albumin; DAPI: 4',6-diamidino-2-phenylindole; ELISA: enzyme-linked immunosorbent assay; FBS: fetal bovine serum; HPRT 1; hypoxanthine phosphoribosyltransferase 1; ILs: interleukins; LDH: lactate dehydrogenase; MAPK: mitogen-activated protein kinase; MOI: multiplicities of infection; NLRs: Nucleotide-binding oligomerization domain (NOD)-like receptors; NOD: Nucleotide-binding oligomerization domain; PBS: phosphate buffer saline; PCR: polymerase chain reaction; qPCR: quantitative polymerase chain reaction;

Declarations

Ethics approval and consent to participate

Not applicable.

Consent for publication

Not applicable.

Availability of data and materials

All data generated or analyzed during the present study are included in this published article.

Competing interests

The authors declare that they have no competing interests.

Funding

This work was supported by Basic Science Research Program through the National Research Foundation of Korea (NRF) funded by the Ministry of Science, ICT and Future Planning (NRF-2019R1A2C1088346) at Chungnam National University, and the National Natural Science Foundation of China (81771612 and 81971389), the Natural Science Foundation of Guangdong Province (2019A1515011888 and 2019A1515011715), the Characteristic Innovation Projects of Guangdong Universities (2018KTSCX081, 2018KTSCX079).

Authors' contributions

JQC, FFG, WW, JHQ and YHL designed and conceived the experiments. JQC, FFG, WW, CL, ZP, JS, HW, CH and SHL carried out the experiments. JQC, FFG, WW, JHQ and YHL performed the data analysis. JQC, JHQ and YHL LL, XW drafted and revised the manuscript. All authors read and approved the final manuscript.

References

1. Robert-Gangneux F, Dardé ML. Epidemiology of and diagnostic strategies for toxoplasmosis. Clin Microbiol Rev. 2012;25:264-96.
2. Harker K, Ueno N, Lodoen M. *Toxoplasma gondii* dissemination: a parasite's journey through the infected host. Parasit Immunol. 2015;37:141-9.
3. Peterson LW, Artis D. Intestinal epithelial cells: regulators of barrier function and immune homeostasis. Nat Rev Immunol. 2014;14:141-53.
4. Pifer R, Yarovinsky F. Innate responses to *Toxoplasma gondii* in mice and humans. Trends Parasitol. 2011;27:388-93.
5. Olive C. Pattern recognition receptors: sentinels in innate immunity and targets of new vaccine adjuvants. Expert Rev Vaccines. 2012;11:237-56.
6. Yarovinsky F. Toll-like receptors and their role in host resistance to *Toxoplasma gondii.* Immunol Letters. 2008;119:17-21.
7. Franchi L, Warner N, Viani K, Nuñez G. Function of Nod-like receptors in microbial recognition and host defense. Immunol Rev. 2009;227:106-28.
8. Nagyőszi P, Nyúl-Tóth Á, Fazakas C, Wilhelm I, Kozma M, Molnár J, et al. Regulation of NOD-like receptors and inflammasome activation in cerebral endothelial cells. J Neurochem. 2015;135:551-64.
9. Shaw MH, Reimer T, Sanchez-Valdepenas C, Warner N, Kim YG, Fresno M, et al. T cell-intrinsic role of Nod2 in promoting type 1 immunity to *Toxoplasma gondii.* Nat Immunol. 2009;10:1267–1274.
10. Witola WH, Mui E, Hargrave A, Liu S, Hypolite M, Montpetit A, et al. NALP1 influences susceptibility to human congenital toxoplasmosis, proinflammatory cytokine response, and fate of *Toxoplasma gondii*-infected monocytic cells. Infect Immun. 2011;79:756–766.
11. Gorfu G, Cirelli KM, Melo MB, Mayer-Barber K, Crown D, Koller BH, et al. Dual role for inflammasome sensors NLRP1 and NLRP3 in murine resistance to *Toxoplasma gondii.* mBio. 2014;5:e01117-13.
12. Chu JQ, Shi G, Fan YM, Choi IW, Cha GH, Zhou Y, et al. Production of IL-1beta and Inflammasome with Up-Regulated Expressions of NOD-Like Receptor Related Genes in *Toxoplasma gondii*-Infected THP-1 Macrophages. Korean J Parasitol. 2016;54:711-717.
13. Strowig T, Henao-Mejia J, Elinav E, Flavell R. Inflammasomes in health and disease. Nature. 2012;481:278-86.
14. Vladimer GI, Weng D, Paquette SWM, Vanaja SK, Rathinam VA, Aune MH, et al. The NLRP12 inflammasome recognizes *Yersinia pestis*. Immunit. 2012;37:96-107.
15. Clay GM, Sutterwala FS, Wilson ME. NLR proteins and parasitic disease. Immunol Res. 2014;59:142-52.
16. Quan JH, Huang R, Wang Z, Huang S, Choi I-W, Zhou Y, et al. P2X7 receptor mediates NLRP3-dependent IL-1β secretion and parasite proliferation in Toxoplasma gondii-infected human small intestinal epithelial cells. Parasit Vectors. 2018;11:1-10.
17. Hao Chen H, Yang D, Han F, Tan J, Zhang L, Xiao J, et al. The Bacterial T6SS Effector EvpP Prevents NLRP3 Inflammasome Activation by Inhibiting the Ca 2+-Dependent MAPK-Jnk Pathway. Cell Host Microbe. 2017;21:47-58.
18. Zhou Z, Li H, Tian S, Yi W, Zhou Y, Yang H, et al. Critical roles of NLRP3 inflammasome in IL-1beta secretion induced by *Corynebacterium pseudotuberculosis* in vitro. Mol Immunol. 2019;116:11-17.
19. Fenini G, Grossi S, Gehrke S, Beer H-D, Satoh TK, Contassot E, et al. The p38 mitogen-activated protein kinase critically regulates human keratinocyte inflammasome activation. J Invest Dermatol. 2018;138:1380-90.
20. Chen TTW, Cheng PC, Chang KC, Cao JP, Feng JL, Chen CC, et al. Activation of the NLRP3 and AIM2 inflammasomes in a mouse model of *Schistosoma mansoni* infection. J Helminthol. 2019;94:e72.
21. Li L, Wang XC, Gong PT, Zhang N, Zhang X, Li S, et al. ROS-mediated NLRP3 inflammasome activation participates in the response against Neospora caninum infection. Parasit Vectors. 2020;13:449.
22. Xie Q, Shen W-W, Zhong J, Huang C, Zhang L, Li J. Lipopolysaccharide/adenosine triphosphate induces IL-1β and IL-18 secretion through the NLRP3 inflammasome in RAW264. 7 murine macrophage cells. Int J Mol Med 2014;34(1):341-9.
23. Feng H, Gu J, Gou F, Huang W, Gao C, Chen G, et al. High glucose and lipopolysaccharide prime NLRP3 inflammasome via ROS/TXNIP pathway in mesangial cells. J Diab Res. 2016;2016:6973175.

24. Wang S, Wang Z, Gu Y, Li Z, Li Z, Wei F, et al. *Toxoplasma gondii* mitogen-activated protein kinases are associated with inflammasome activation in infected mice. Microbes Infect. 2016;18:696-700.

Figures

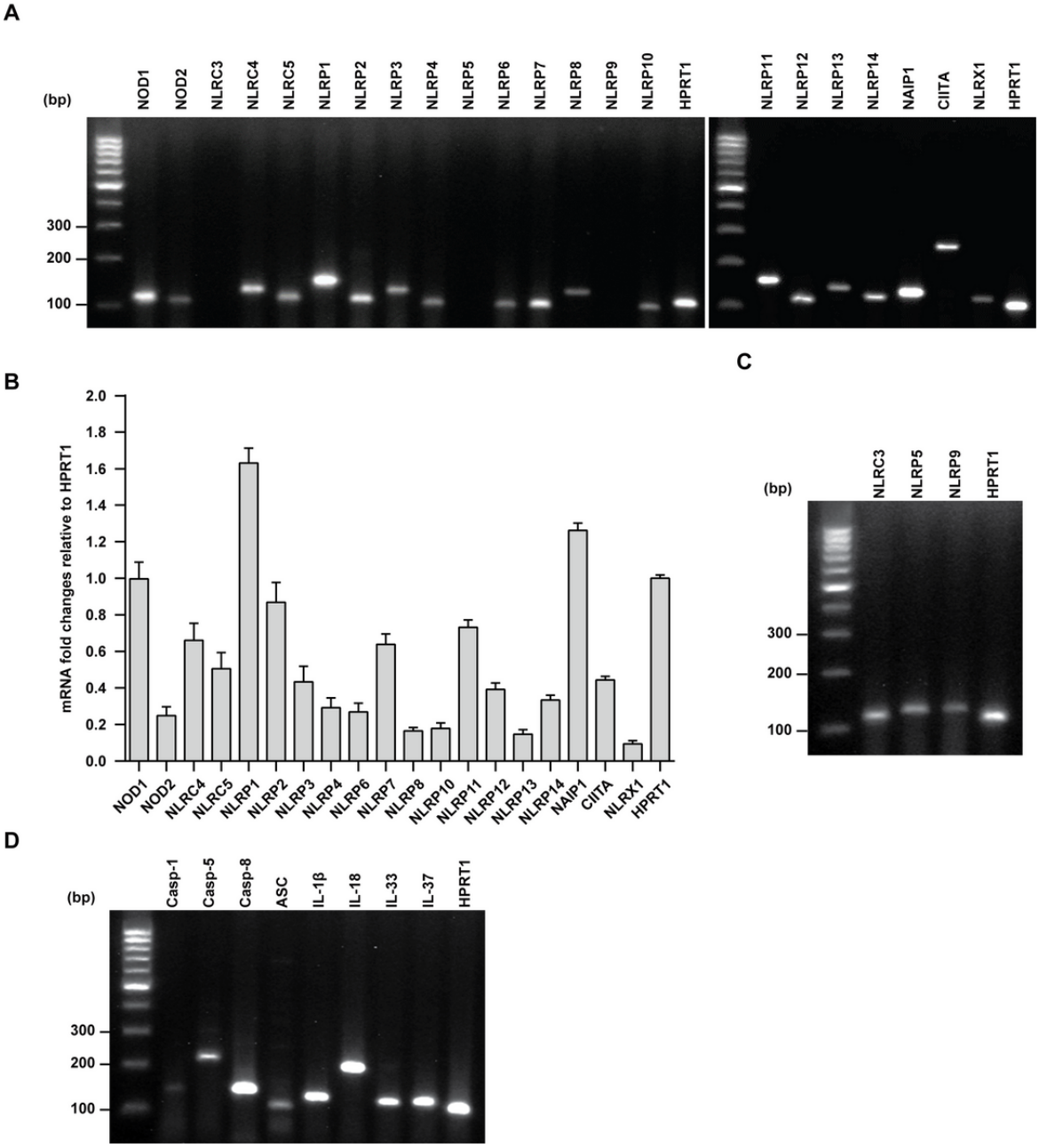

Figure 1

Expression of nucleotide-binding oligomerization domain-like receptors (NLRs), inflammasome components, and caspase-cleaved interleukins (ILs) in human small intestinal epithelial (FHs 74 Int) cells. Total RNA isolated from the untreated cells was examined by polymerase chain reaction (PCR) for mRNA expression of different genes. (A) Expression of NLR mRNAs in FHs 74 Int cells. (B) Expression of the NLR mRNAs in FHs 74 Int cells compared to HPRT 1. (C) Positive controls for primer functionality using human acute monocytic leukemia cell line (THP-1). (D) Inflammasome components and caspase-cleaved ILs expressed in FHs 74 Int cells. Images shown are representatives of five independent experiments.

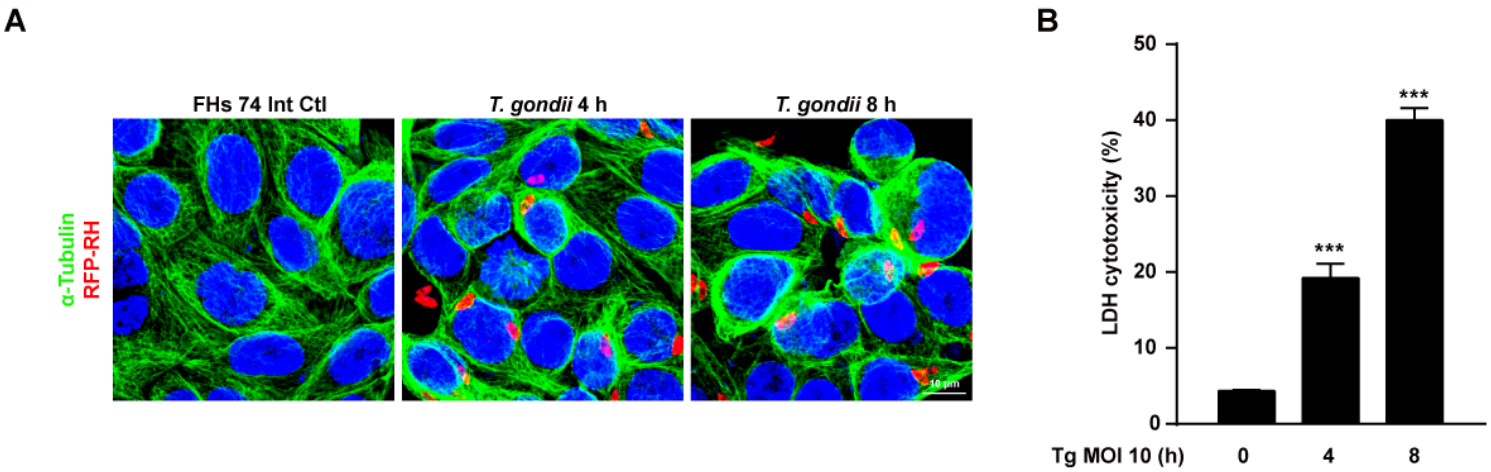

Figure 2

Effects of T. gondii infection on cell morphology and cytotoxicity of FHs 74 Int cells. FHs 74 Int cells were infected with RFP-RH T. gondii strain at a multiplicity of infection (MOI) of 10 for 0, 4, and 8 h. (A) Cells fixed and stained with α-Tubulin (green) and nuclei stained with DAPI (blue) were observed by confocal microscopy. (B) Lactate dehydrogenase level in the media, which is related with cell death, was measured in FHs 74 Int cells infected with T. gondii at a MOI of 10 for 0, 4, and 8 h. The percentage of cytotoxicity was calculated. Horizontal lines in each group represent mean ± standard deviation value of at least 3 independent experiments. ***P< 0.001, as compared to the control group.

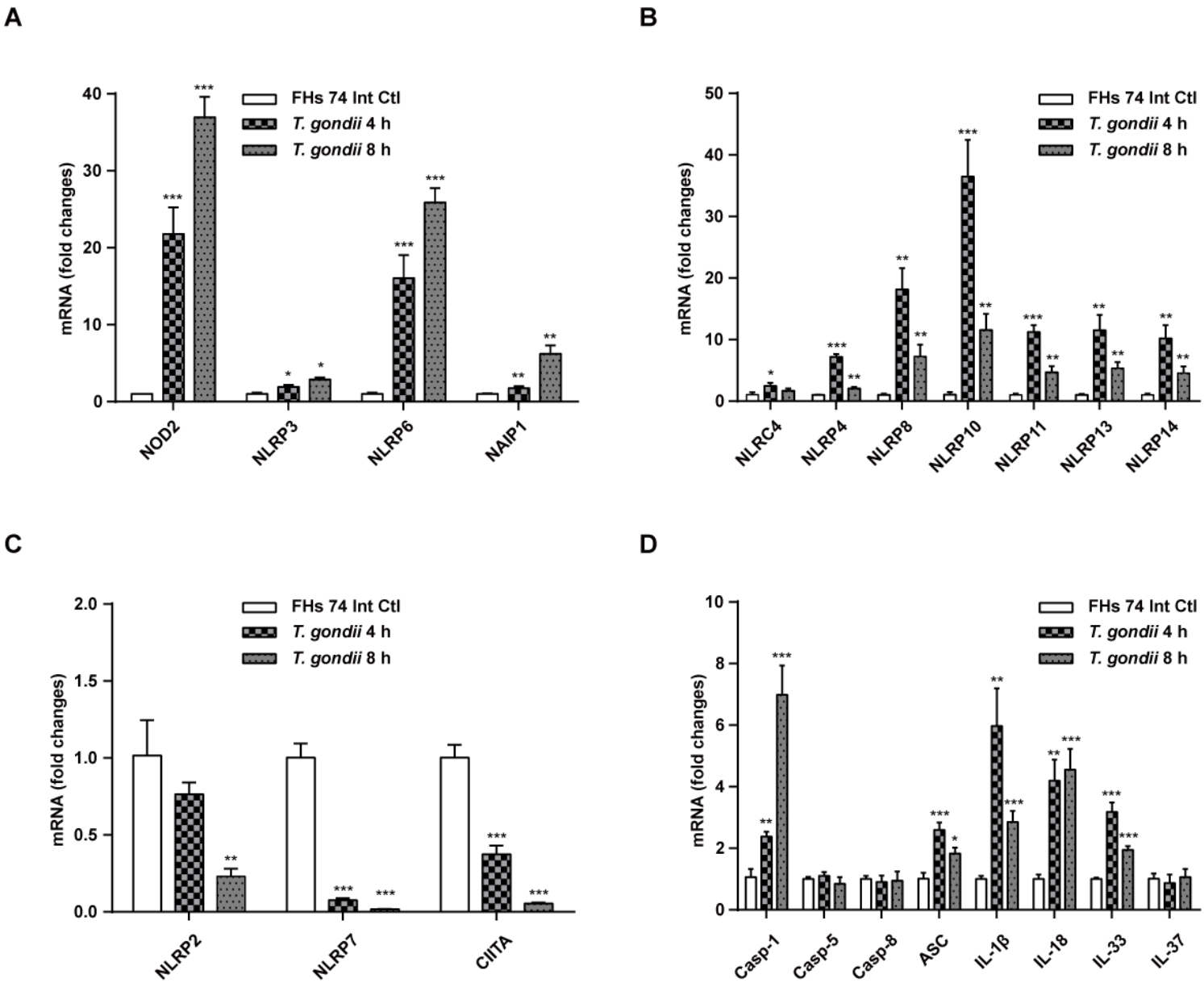

Figure 3

Induction of NLRs, inflammasome components, and caspase-cleaved ILs in response to T. gondii infection in FHs 74 Int cells. FHs 74 Int cells were infected with RFP-RH T. gondii strain at a MOI of 10 for 0, 4, and 8 h. (A–D) Expression of the NLR mRNAs, inflammasome components, and caspase-cleaved ILs in FHs 74 Int cells. Each PCR was carried out with three parallels. *P< 0.05, **P< 0.01, ***P< 0.001 compared to control.

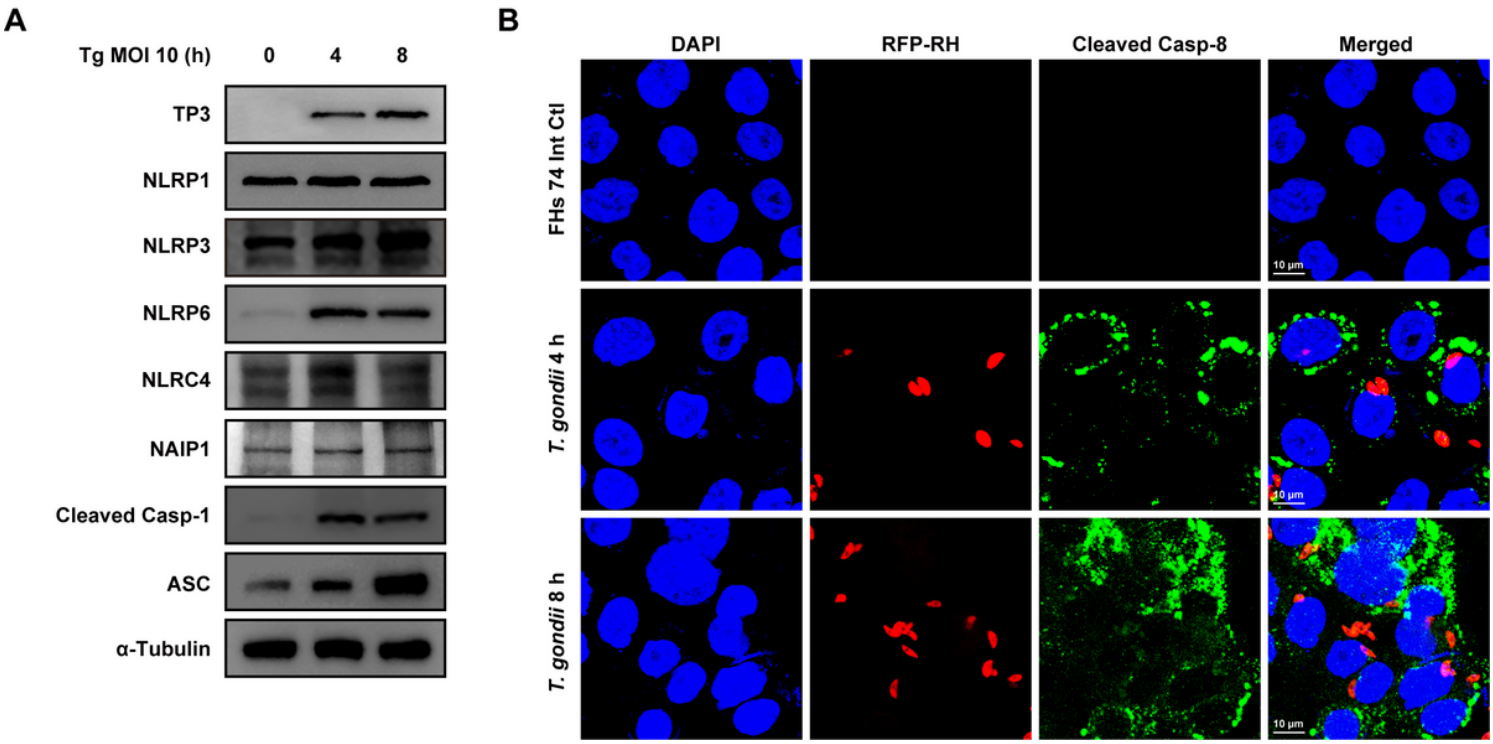

Figure 4

Expression of NLR family members, NLRP1, NLRP3, NLRP6, and NLRC4 inflammasome components in response to T. gondii infection in human small intestinal epithelial (FHs 74 Int) cells. (A) FHs 74 Int cells were infected with T. gondii at a MOI of 10 for 0, 4, and 8 h. Expression of NLRP1, NLRP3, NLRP6, and NLRC4 inflammasome component proteins were detected by western blot analysis; α-tubulin was used as the loading control. (B) FHs 74 Int cells were fixed and probed against cleaved caspase-8 (green). The cells were counterstained with 4',6-diamidino-2-phenylindole (blue) and visualized using confocal microscopy. All data shown are representative of three independent experiments with similar results.

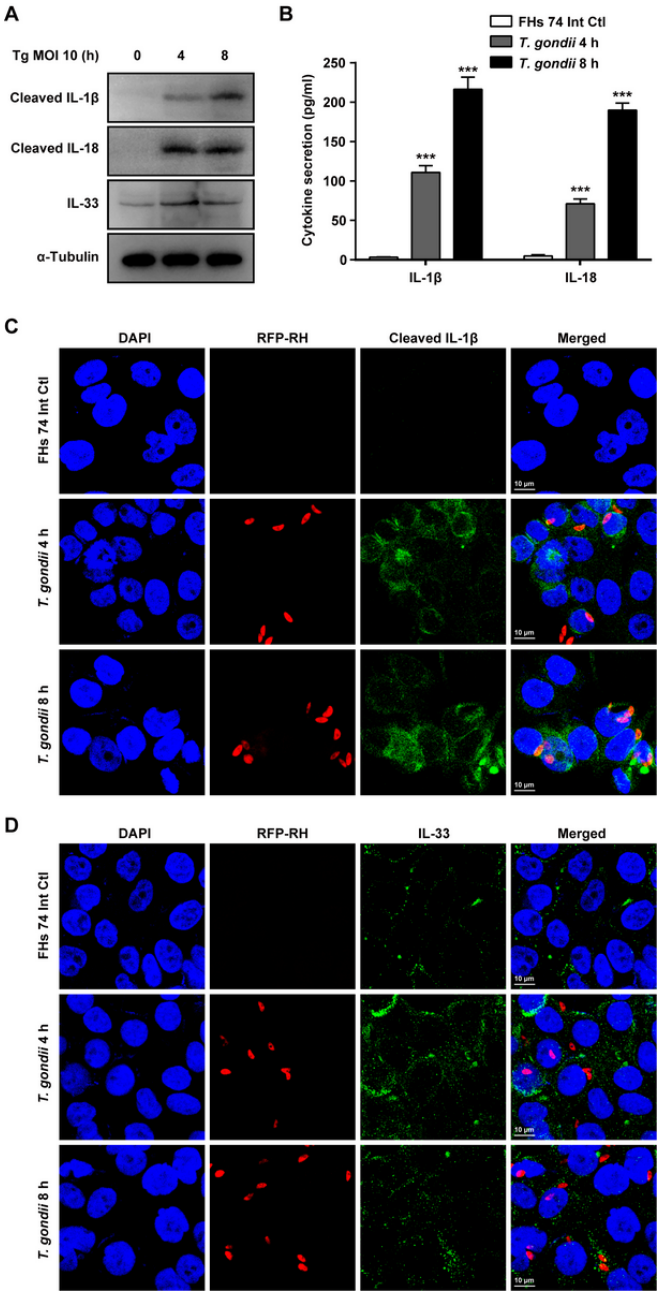

Figure 5

Caspase-cleaved ILs in response to T. gondii infection in FHs 74 Int cells. (A) FHs 74 Int cells were infected with T. gondii at a MOI of 10 for 0, 4, and 8 h. Protein levels of ILs were detected by western blot analysis; α-tubulin was used as the loading control. (B) IL-1β and IL-18 protein levels in the culture medium of FHs 74 Int cells after T. gondii infection were measured by ELISA. Graphs show quantified results in pg/ml as mean ± standard error. ***P< 0.001 compared to control. (C, D) FHs 74 Int cells were fixed and probed against cleaved IL-1β and IL-33. The cells were counterstained with 4',6-diamidino-2-phenylindole (blue) and visualized using confocal microscopy. All data shown are representative of three independent experiments with similar results.

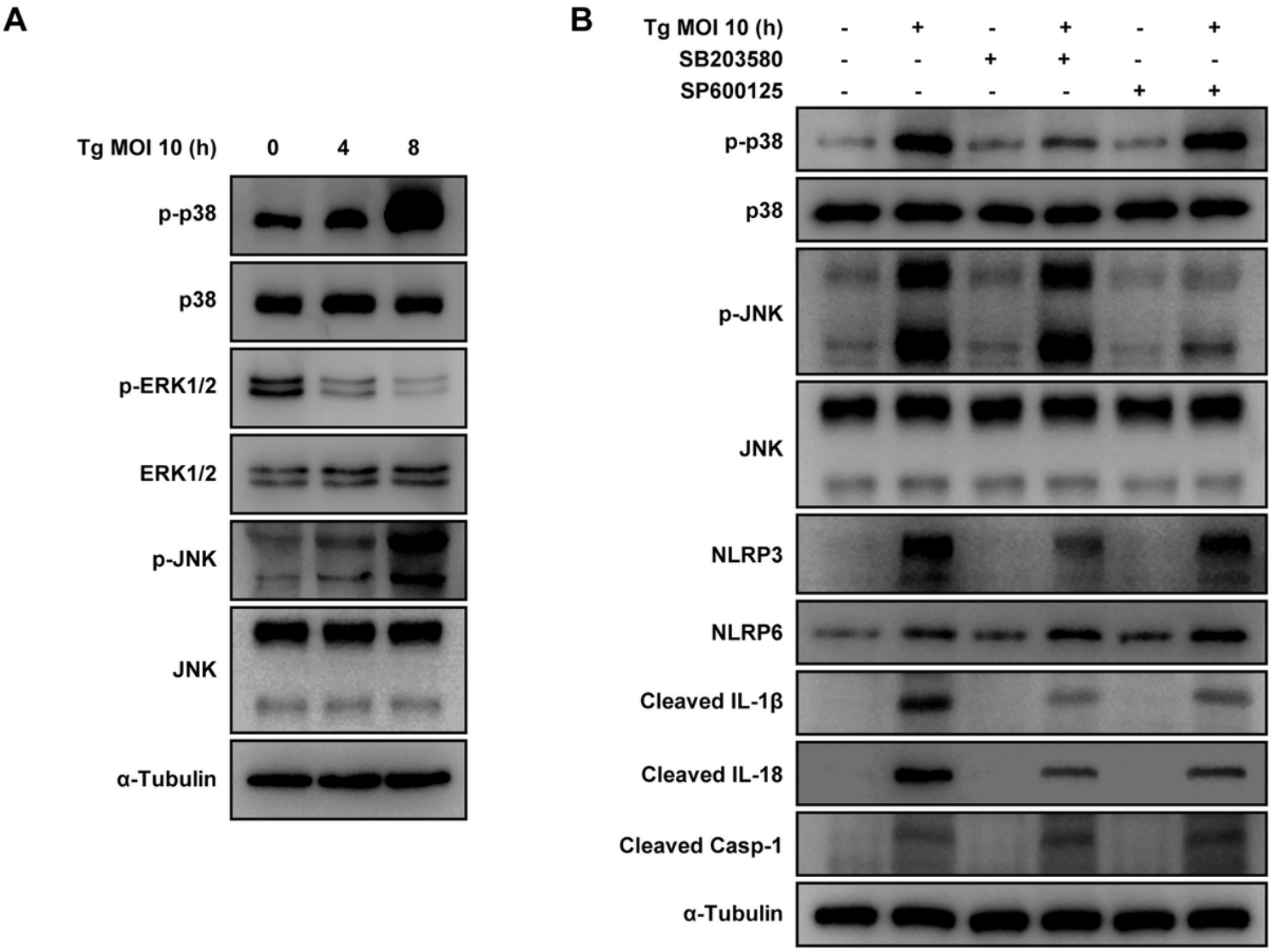

Figure 6

Signaling pathways involved in the regulation of NLRP3 and NLRP6 inflammasome components. (A) FHs 74 Int cells were infected with T. gondii at a MOI of 10 for the indicated time periods. Activation of mitogen-activated protein kinase (MAPK) subsets was evaluated by western blotting. (B) FHs 74 Int cells were preincubated with the SB203580 (p38 MAPK inhibitor) and SP600125 (JNK inhibitor), respectively for 2 h and then infected with T. gondii at a MOI of 10 for 8 h. The indicated protein levels were then evaluated by western blot. Anti-α-tubulin was used as the internal control. Similar results were obtained in three independent experiments.

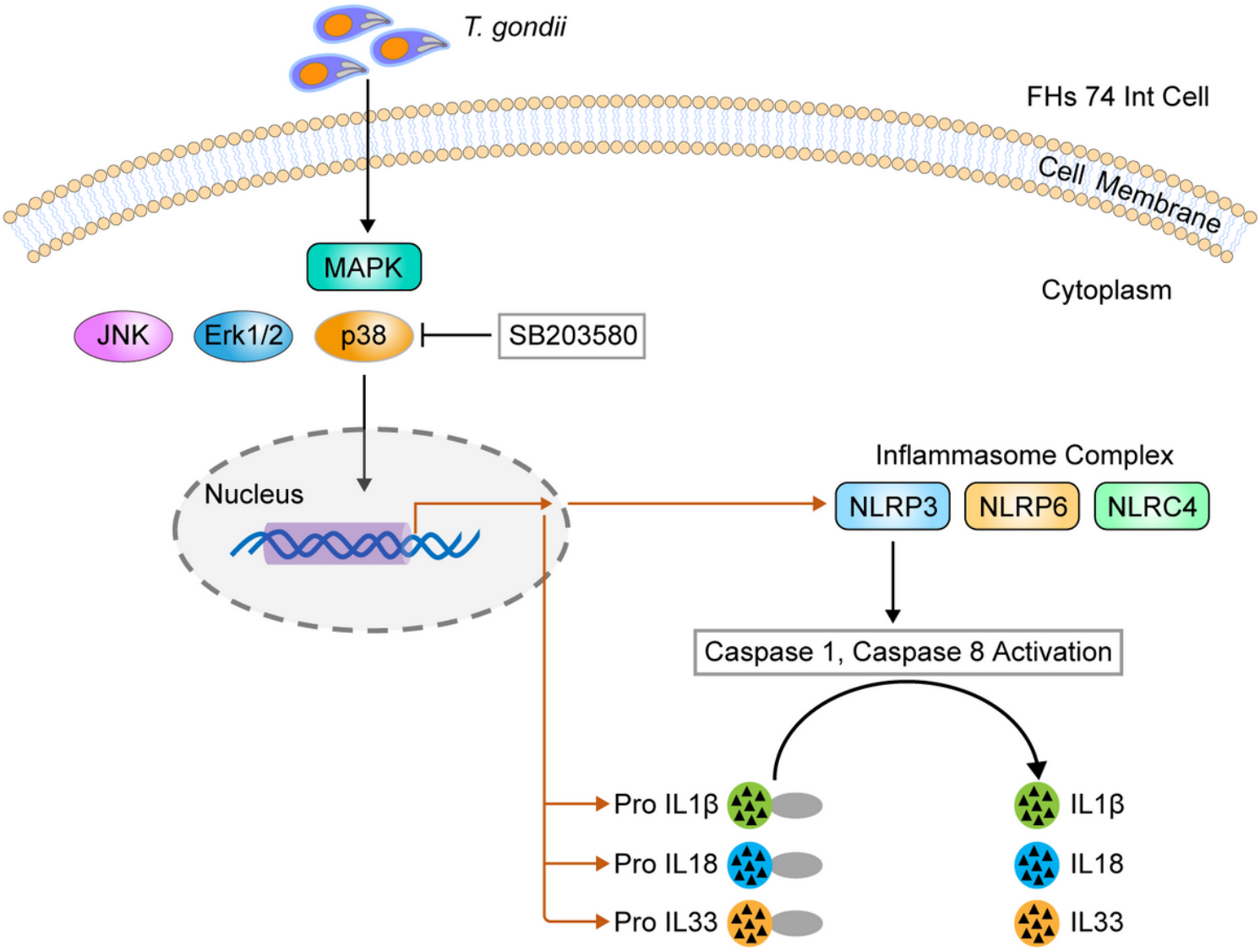

Figure 7

Schematic model of NLRP3 inflammasome activation in T. gondii-infected FHs 74 Int cells. T. gondii activates the p38 MAPK pathway in small intestinal epithelial cells and subsequently upregulating protein expression and promoting the formation of the NLRP3 inflammasome. The NLRP3 inflammasome cleaves pro-IL-1β, pro-IL-18 and pro-IL-33 to become active IL-1β, IL-18 and IL-33, which ultimately induces cytotoxicity of FHs 74 Int cells.